

Modeling the Spread of the Emerald Ash Borer

Brandon Bergerud

December 9, 2018

Introduction

One of the unintended consequences of increased globalization has been the accidental introduction of invasive species into new environments. The lack of predators often leads to an explosive growth in the population that threatens native species and habitats [Mooney and Cleland, 2001]. The iconic elm tree has largely been extinguished in Europe and America due to the spread of an Asian fungi [Santini and Faccoli, 2015], while the emerald ash borer (EAB) is now decimating vast numbers of American ash trees [Cappaert et al., 2005, Herms and McCullough, 2014, Poland and McCullough, 2006].

Originally native to eastern Asia, the invasive presence of EABs in North America was first discovered near Detroit, Michigan in 2002 and has been spreading throughout eastern portions of Canada and the United States at a rate of 20 km/year (Figure 1). On local scales, EABs tend to naturally spread at a rate of only a few kilometers per year, but human assisted means (such as transporting infested ash and hitchhiking on vehicles) has greatly exacerbated the spread of EAB.

Researchers have increasingly turned to computer simulations to help better understand the spread of invasive species and help forecast areas of increased risk. A common approach over large areas has been the use of cellular models. BenDor et al. [2006] used such models to examine the effectiveness of firewood quarantines on the spread of EAB in DuPage County, Illinois, while Prasad et al. [2009] generated maps of EAB risk levels in Ohio. At the city level, agent-based models have been employed to better understand their dispersal behavior and infestation tendencies [Anderson and Dragicevic, 2015].

This project aims to perform a similar goal by modeling the spread of EAB through computer simulations and comparing the results with real-world observations. One of the major issues with simulations is that much of the necessary data is government owned, and thus special permission must be granted to gain

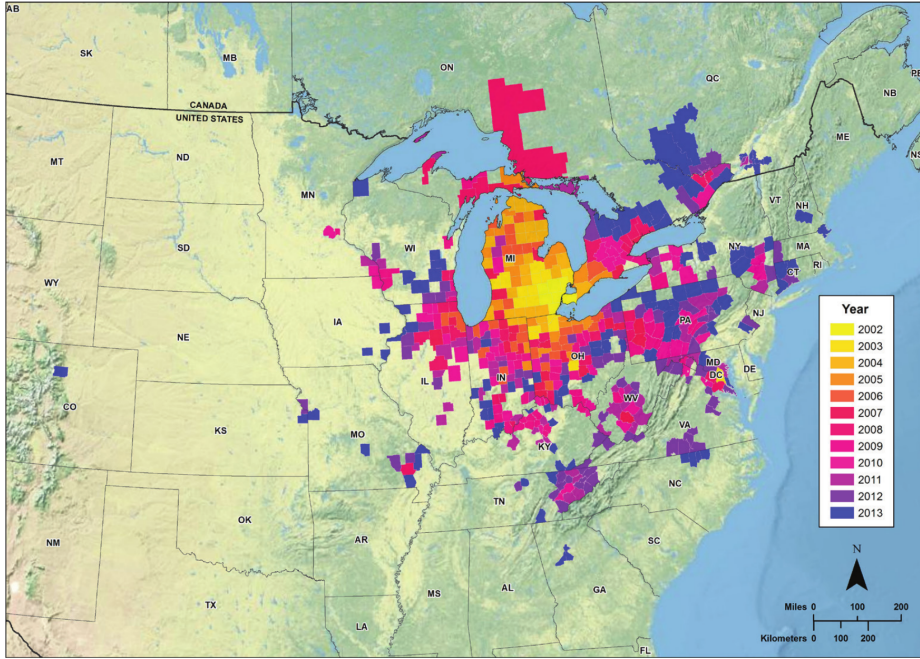


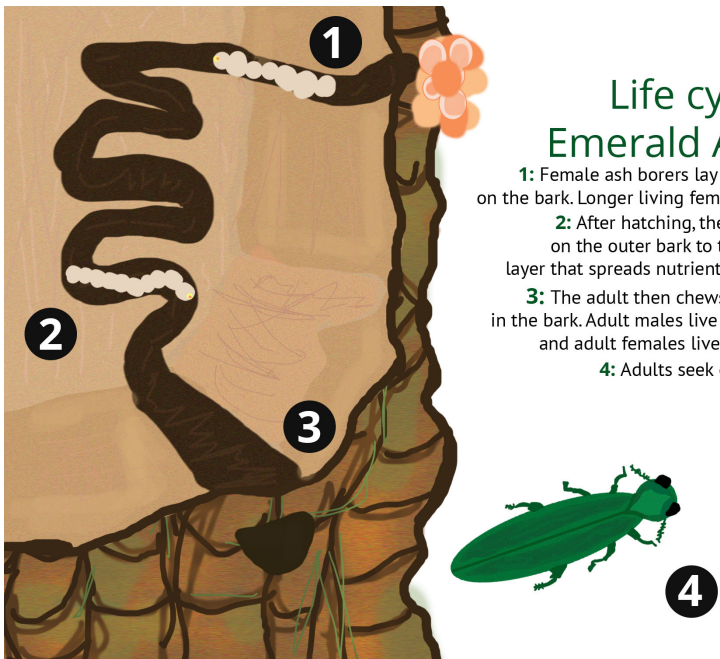
Figure 1: Initial detection of EAB in North America. Figure from [Haack et al. \[2015\]](#)

access to the data. Access to the Cedar Rapids Street Tree inventory was provided, which will serve as the dataset with which to model the spread of EAB through agent-based modeling within the Julia programming language [[Bezanson et al., 2012](#)]. While this dataset won't allow for a direct comparison with the spread of EAB, other parameters can be compared with observations from other areas, such as larval densities, the number of exit holes, and the dispersal rate.

EAB Life Cycle

The life cycle of an emerald ash borer is illustrated in Figure 2. Adult EABs begin emerging in late May or early June, with females usually living for 21 – 25 days (males just 13 days), although instances of up to 6 weeks have been observed [Buck, 2015]. After emergence, EABs forage on ash leaves for a week or two to gather strength before mating. After mating, females deposit eggs in bark crevices, usually just a single egg at a time, but lay around 40 – 70 eggs over the course of their life.

Larvae begin to hatch within 1 – 2 weeks and bore through the bark to feed on the interior phloem (which acts as the tree’s nutrient highway). In late October, larvae bore into the outer sapwood and become inactive until April, at which point they begin pupating and develop into an adult beetle. Once complete, they emerge from the tree by boring D-shaped exit holes and the cycle begins anew [Herms and McCullough, 2014].



Life cycle of the Emerald Ash Borer

1: Female ash borers lay between 40 - 70 eggs on the bark. Longer living females can lay up to 200.

2: After hatching, the larvae begin feeding on the outer bark to the phloem, the tissue layer that spreads nutrients throughout the tree.

3: The adult then chews a D-shaped exit hole in the bark. Adult males live an average of 13 days and adult females live an average of 21 days.

4: Adults seek out new trees and the process begins again.

Figure 2: Life cycle of EAB. Figure from [Medill](#)

Data

This project makes use of the Cedar Rapids Street Tree inventory, which is current as of 29 March 2017. This inventory contains the location of about 60,000 trees, while also providing information such as the tree type, condition, and the diameter at breast height (DBH).

This data was queried to select ash trees that were alive and whose DBH was greater than 5 cm. The later requirement comes from observations that EABs generally don't attack such small trees [Anderson and Dragicevic, 2015]. Only four ash are excluded based on this condition. The resulting spatial distribution of ash trees is plotted in Figure 3, while the distribution of ash types are shown in Table 1.

Since the surface area is not provided, this must be estimated. McCullough and Siegert [2007] provide a detailed examination of dead ash trees due to EAB and included several fits to a DBH-surface area relationship, such as the one plotted in Figure 4. The following model is adopted for estimating the surface area σ ,

$$\sigma(\text{DBH [cm]}) = 0.0195 \cdot \text{DBH}^2 - 0.0035 \cdot \text{DBH} + 0.0071 \quad [\text{m}^2] \quad (1)$$

Ash Type	Quantity
Blue	25
European	19
Green	5814
White	1186

Table 1: Distribution of ash types in the Cedar Rapids street tree inventory. The one instance of a European mountain ash is not included, as it isn't a true ash. There are 7044 ash trees in total as of 03/29/2017.

Ash Trees in Cedar Rapids

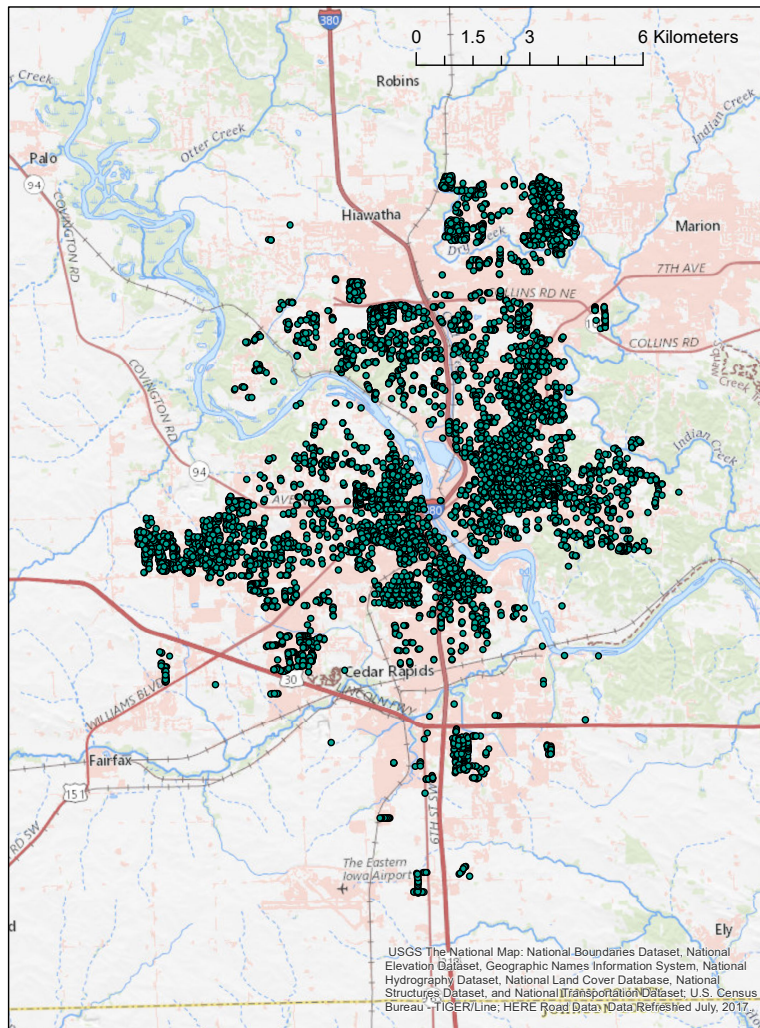


Figure 3: Distribution of 7044 Ash trees in Cedar Rapids.

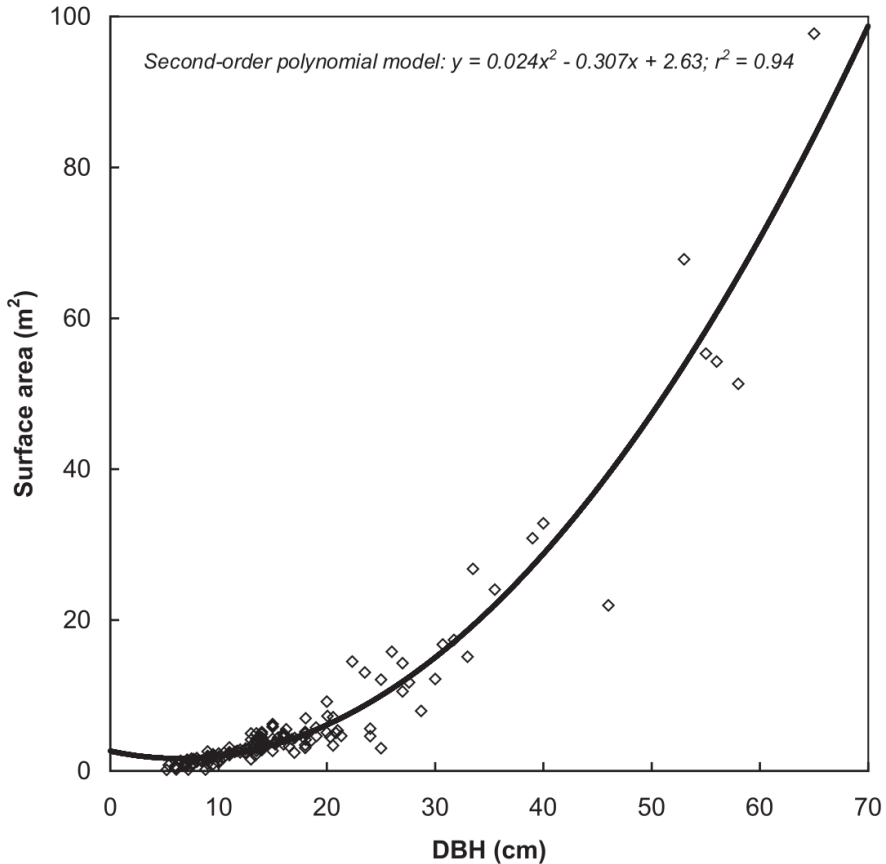


Figure 4: DBH-Surface Area relationship using a second-order polynomial fit.
Figure from [McCullough and Siegert \[2007\]](#).

While this fit was performed using smaller trees with $\text{DBH} \leq 13 \text{ cm}$, there are a couple advantages. It is monotonically increasing for $\text{DBH} > 0 \text{ cm}$, while also having a y-intercept very close to zero. The fit matches up fairly well with the fit provided in Figure 4 and is less likely to be affected by the presence of a few very high leverage observations at large DBH.

Simulation

The model of choice is an agent-based model similar to [Anderson and Dragicevic \[2015\]](#) and is schematically illustrated in Figure 5. The model proceeds as follows:

1. Starting with the tree inventory, one assigns an initial larval infestation from the previous summer.
2. Some of these larvae will die according to deterministic (e.g. density) and random events. These death rates are defined by the user.
3. The larvae that survive these events will emerge from the tree, with the number of days until emergence set by a provided function (should return a non-positive value). The age, status, and tree location of the female beetles is monitored throughout the simulation.
4. The season is simulated until all the females are dead. The first step is to increment the age of each beetle by one day and then update the beetle status to reflect either 1) pupating, 2) foraging, 3) mating, 4) reproducing, or 5) dead.
5. Females that are foraging will be dispersed based on a provided dispersal function. Females that are reproducing will also disperse according to a provided dispersal function, but will then also lay a certain number of eggs at the tree according to a provided function.
6. The egg counts are kept track of in the tree inventory, and after the season ends the tree is then tested to see if it is dead according to the provided function. This could be generalized in the future so that other statuses could be updated.
7. The larvae are then used as a seed for the next season.

Day		Status		Day
0	<	Foraging	\leq	7
7	<	Mating	\leq	10
10	<	Reproducing	\leq	22
22	<	Dead		

Table 2: Status of a female emerald ash borer based on its age in days.

The assumed age-status relationship is illustrated in Table 2, and closely follows that of [Anderson and Dragicevic \[2015\]](#). The female adult beetles are initialized to have an age of zero.

Larvae are known to be subject to population related deaths. When larval densities are large (> 300 larvae / m^2), the death rate is nearly universal [[McCullough and Siegert, 2007](#)]. The logistic death rate in Figure 7 is adopted, which is similar to the one adopted by [BenDor et al. \[2006\]](#) (particularly Figure 5). The inflection point occurs at $\rho_0 = 150$ larvae / m^2 with a spread of $\sigma = 25$ larvae / m^2 – that is, the larval density ρ is transformed according to

$$x = \frac{\rho - \rho_0}{\sigma} \quad (2)$$

and then passed into a standard logistic function.

The main predator of EAB larvae are woodpeckers, which can occasionally lead to large larval die-offs, as illustrated in Figure 6 for 24 Michigan sites. Following the observed street tree deaths, a random death rate between 0 and 0.6 is sampled and applied to each infested tree.

EABs are known to have host tree preferences. These include preferring trees that are stressed or are already infested. EABs tend to have equal preference for white and green ash, while preferring blue ash the least [[Anulewicz et al., 2008](#), [Rebek et al., 2008](#)]. Distinguishing between the various weighting factors, however, requires some dataset with which to compare; otherwise, the number of variables becomes rather large. A simple dispersal model is therefore adopted where each tree is assigned a probability weight

$$w \propto \frac{\sigma}{d_*^\chi} \quad (3)$$

where σ is the surface of the tree, χ is a power index, and d_* is a modified

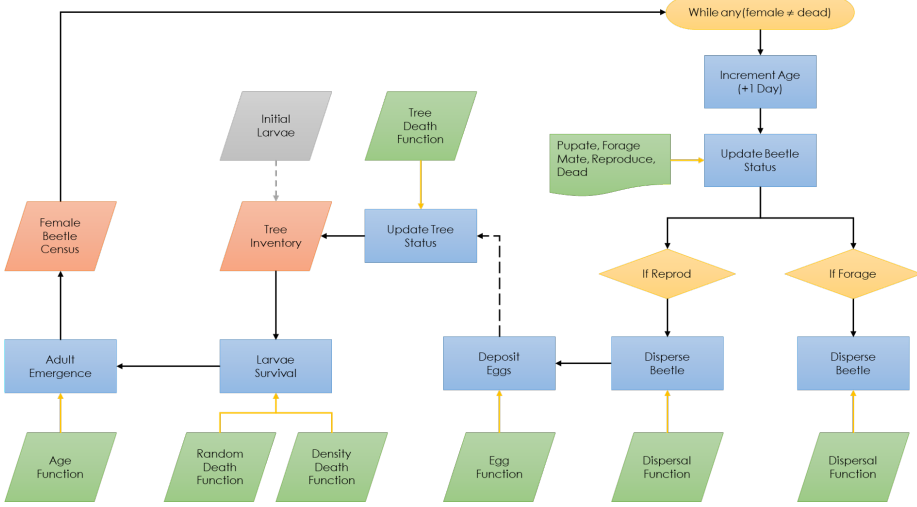


Figure 5: Schematic of the simulation model.

distance given by

$$d_{\star} = \begin{cases} \sqrt{d^2 + \epsilon^2} & d < 2.8 \text{ km} \\ \infty & d > 2.8 \text{ km or dead} \end{cases} \quad (4)$$

where $\epsilon = 10$ meters provides a buffer to avoid division by zero. The 2.8 km comes from the estimated distance an EAB can fly in a day [Taylor et al., 2007]. The probabilities are then computed by normalizing over the weights,

$$p_i = \frac{w_i}{\sum_j w_j} \quad (5)$$

Each beetle is then assigned a new tree according to the designated probabilities. Trees are considered dead after three years of infestation.

Reproducing females are modeled as laying between 1 and 10 eggs during each simulation time step with equal probability for each. Thus, the average female will lay around 66 eggs over the course of her lifetime.

Three 5-year seasons of infestation are simulated with different power indices for $\chi \in \{1, 2, 3\}$. For each χ , the same initial tree is infested with 50 larvae to start the simulation and the model progressed through 5 seasons. The number of exit holes (successful emerging adults) is counted, the cumulative larval counts for each tree, as well as the number of years since the tree was first infested. The results are discussed in the next section.

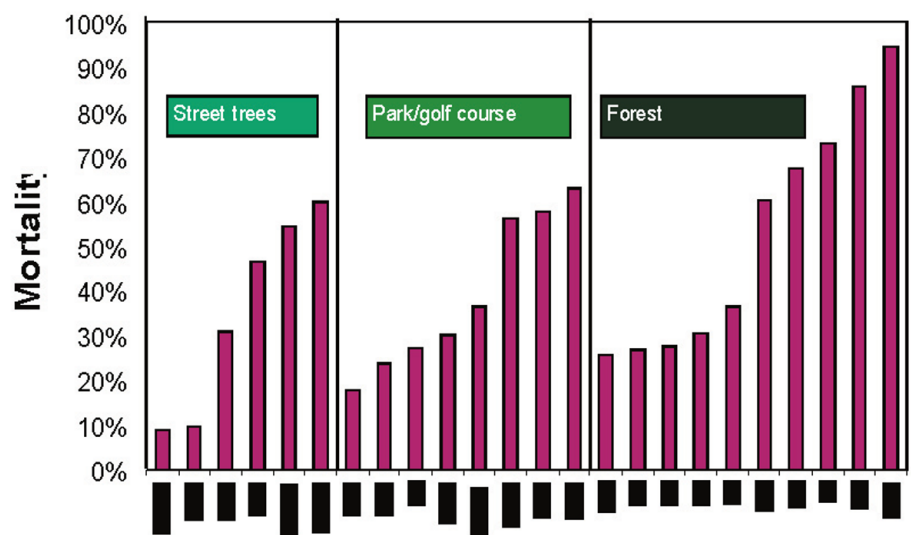


Figure 6: Mean larval mortality at 24 Michigan sites attributed to Woodpeckers.
Figure from [Cappaert et al. \[2005\]](#).

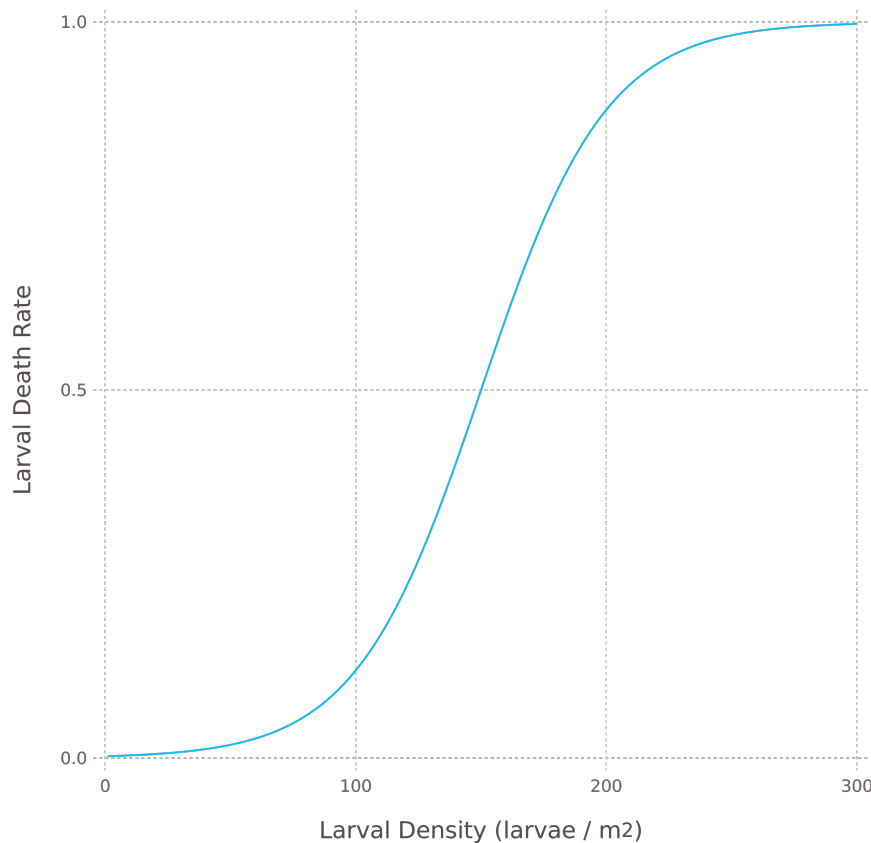


Figure 7: Logistic death rate used for larval densities. The inflection density occurs at 150 larvae / m^2 .

Results

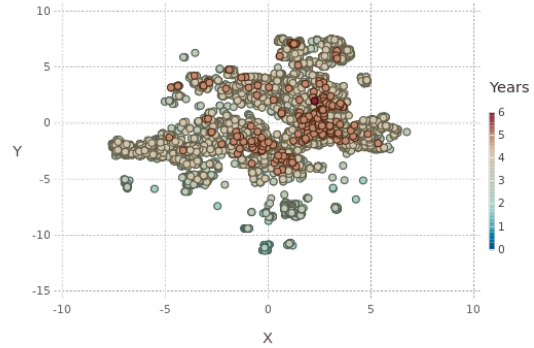
The spatial-temporal distribution of tree infestations is plotted in Figure 8, with the original epicenter indicated in red (6 years) and uninfested trees in dark blue (0 years). Under a power index of $\chi = 1$, all the trees are infested within four years, while a few trees towards the south and west remain uninfested after 5 years when $\chi = 2$. A power index $\chi = 3$ results in a slow diffusion such that most infested trees are within about 2 km of the epicenter by the end of the 5-year simulation.

Considering just the new infestations during each year, their distances from the original epicenter are illustrated in Figure 9. The solid black line represents an average dispersal rate of ~ 2 km/year [Anderson and Dragicevic, 2015]. A power index of $\chi = 1$ most closely matches observed dispersal rates. The excess during year 4 could be due to the limited number of uninfested trees that remain and the more sparse distribution of trees towards the south. Meanwhile, $\chi = 3$ results in an expansion rate that is too slow, while the maximum extent with $\chi = 2$ tends to match the average observed value.

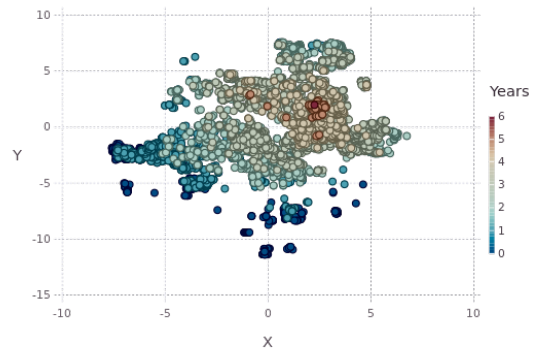
A second observable that can be measured is the number of adult beetles that emerge from each tree. While investigating ash trees killed by EAB, McCullough and Siegert [2007] determined that on average around 90 adults / m^2 successfully emerge from an infested ash tree. There is some variability in these estimates, with larger trees ($DBH > 13$ cm) tending to have around a 30% greater incidence of exit holes compared to smaller trees ($DBH < 13$ cm).

As shown in Figures 10 – 12, the density of exit holes is considerably smaller in the simulation. The simulation shows an upper bound of 100 adults / m^2 , which is comparable to the average observed value. The smaller observed counts could then be a reflection of having too many larvae deposited or too high of a death rate.

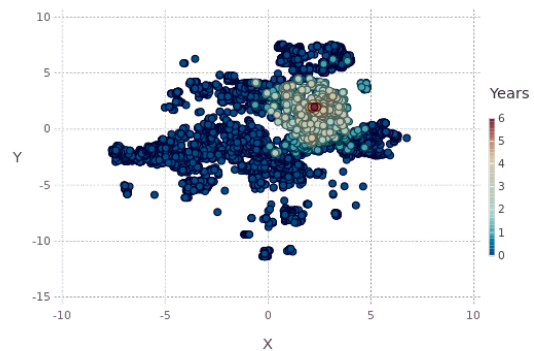
A final check that can be done is to examine the cumulative number of



(a) $\chi = 1$



(b) $\chi = 2$



(c) $\chi = 3$

Figure 8: Years since initial infestation for each tree at the end of the simulation. The original epicenter was a single tree indicated in red (6 years). Uninfested trees are dark blue (0 years).

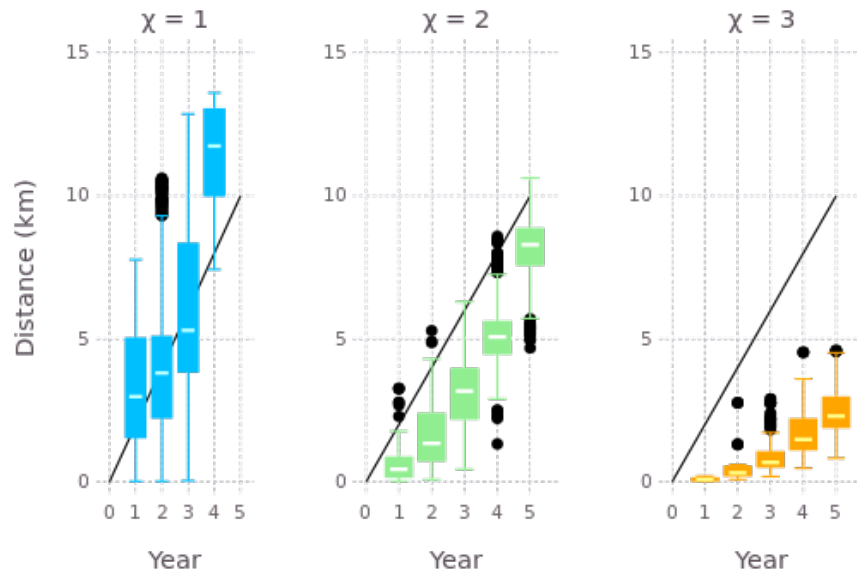


Figure 9: Distribution of new infestations from the original epicenter as a function of the power index χ and the simulation year. The solid black line represents the observed average dispersal rate of ~ 2 km/year [Anderson and Dragicevic, 2015].

larvae that were present. Figures 13 – 15 display this normalized by surface area. Large values of χ tend to result in large numbers of larvae per tree. With heavily infested trees being observed to have densities ranging from 300 to 1000 larvae / m², but suffering large die offs, we can take these as an upper limit to the number of larvae. These densities are exceeded for $\chi \gtrsim 2$, while $\chi = 1$ tends to produce more reasonable numbers, although on the high-side for smaller trees.

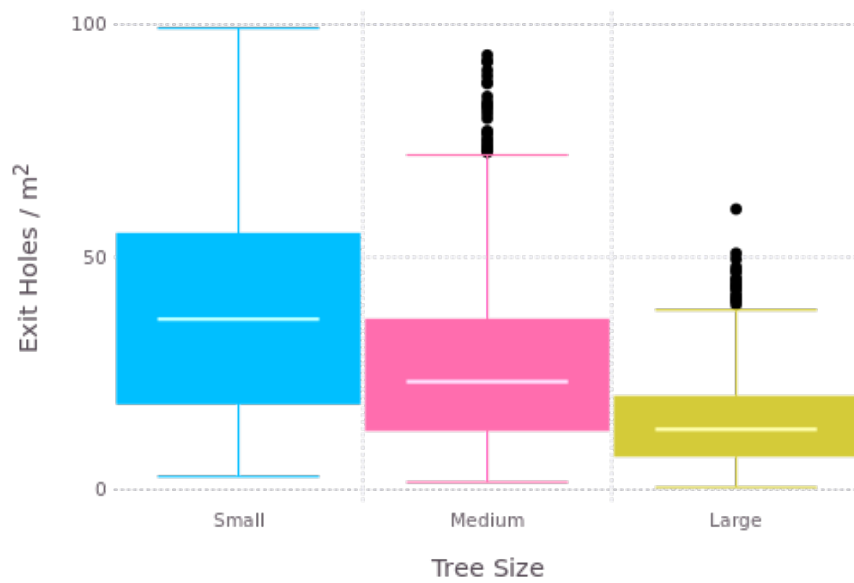
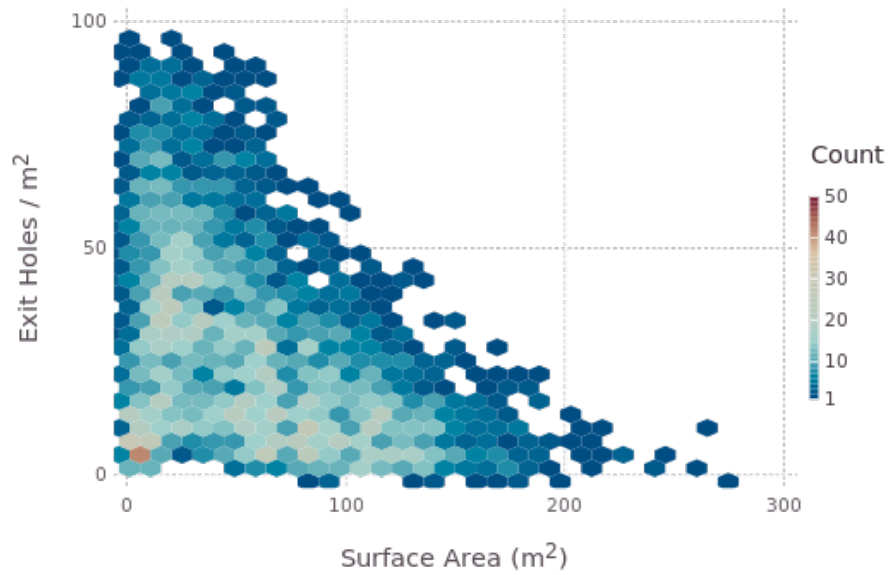


Figure 10: Distribution of exit holes and a tree's surface area when $\chi = 1$. In the bottom figure, trees have been placed into size groups based on their surface area: small, medium ($> 50 \text{ m}^2$), and large ($> 100 \text{ m}^2$).

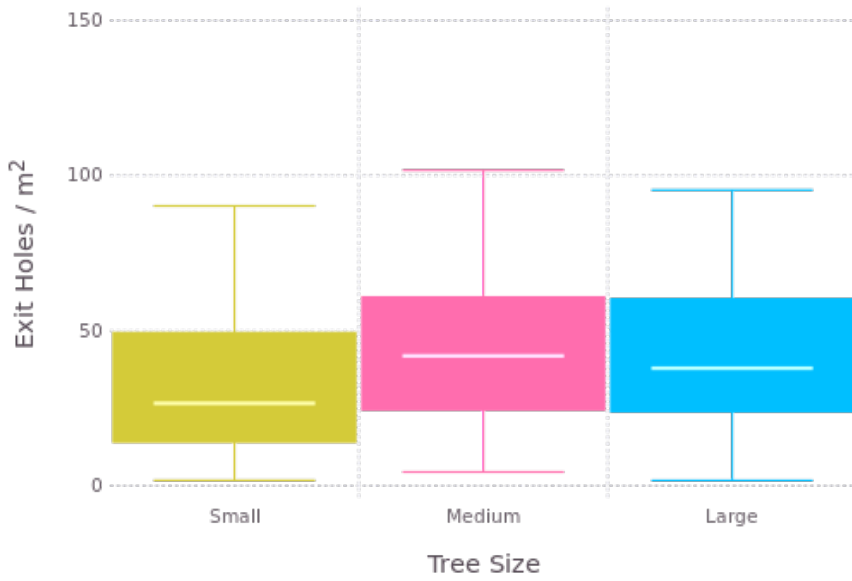
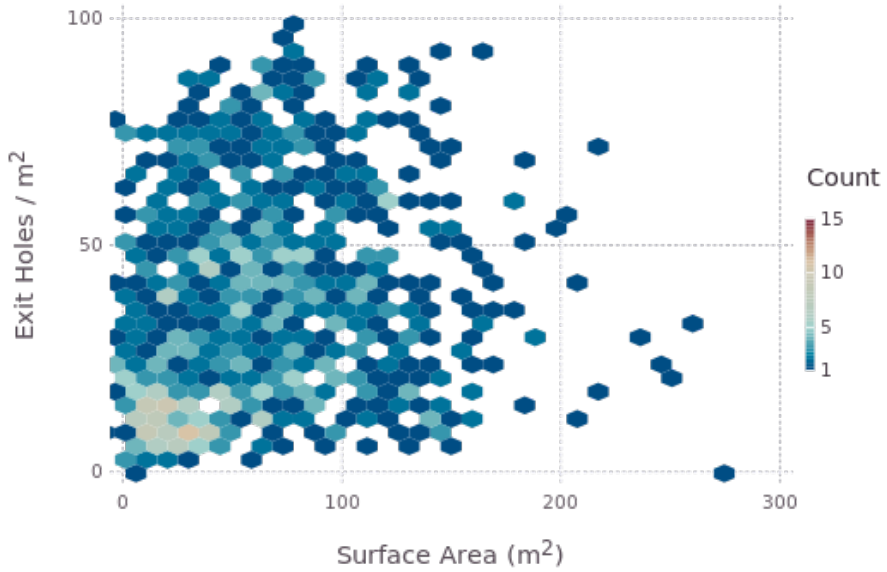


Figure 11: Distribution of exit holes and a tree's surface area when $\chi = 2$. In the bottom figure, trees have been placed into size groups based on their surface area: small, medium ($> 50 \text{ m}^2$), and large ($> 100 \text{ m}^2$).

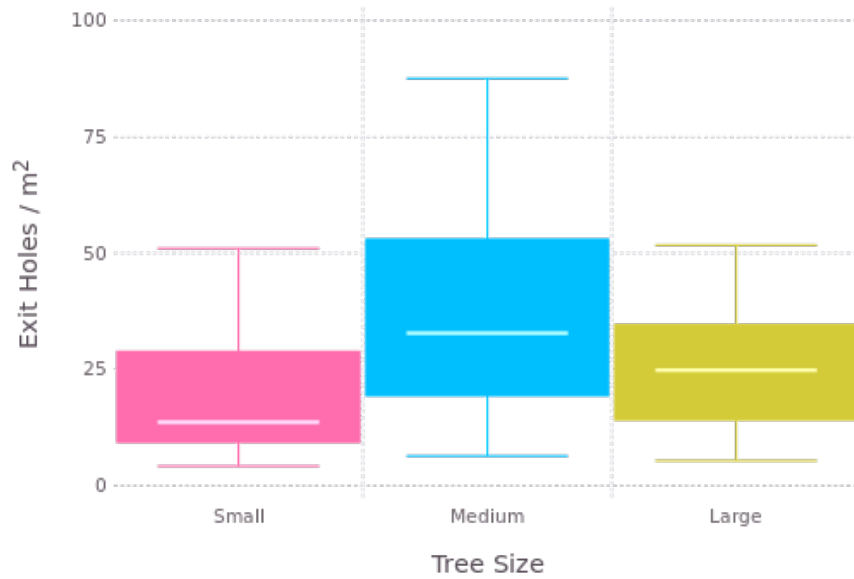
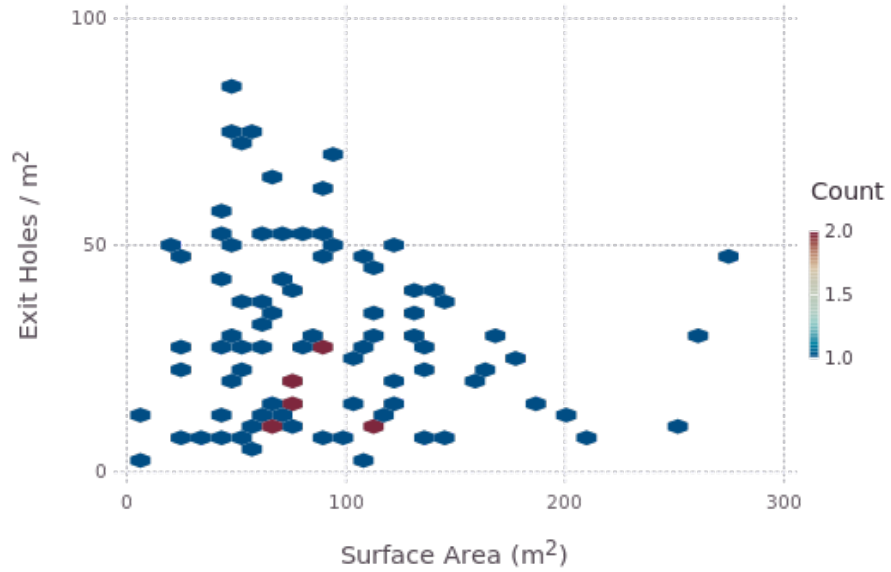


Figure 12: Distribution of exit holes and a tree's surface area when $\chi = 3$. In the bottom figure, trees have been placed into size groups based on their surface area: small, medium ($> 50 \text{ m}^2$), and large ($> 100 \text{ m}^2$).

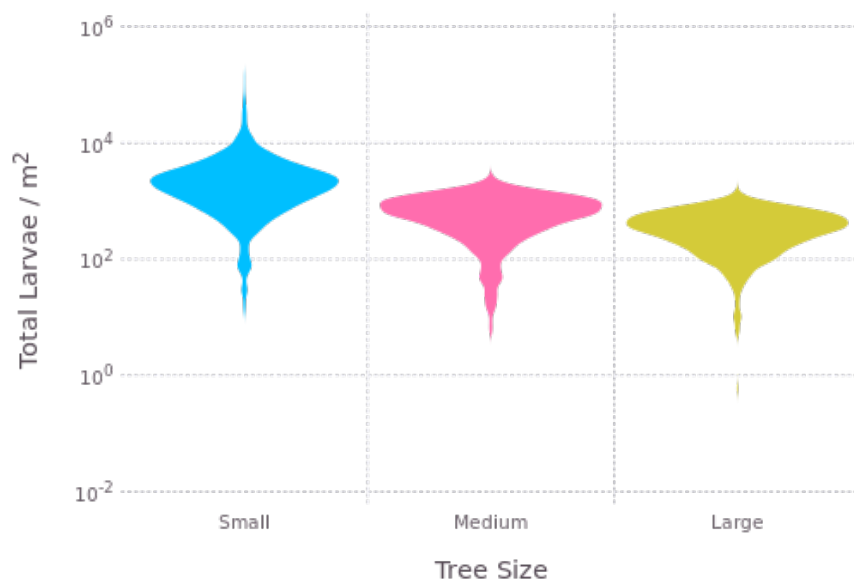
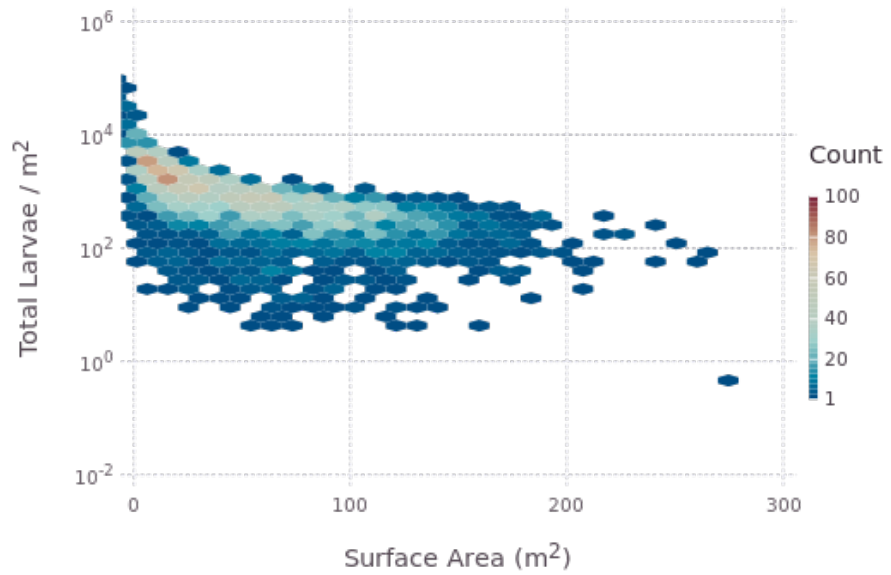


Figure 13: Distribution of the cumulative larval density and a tree's surface area when $\chi = 1$. In the bottom figure, trees have been placed into size groups based on their surface area: small, medium ($> 50 \text{ m}^2$), and large ($> 100 \text{ m}^2$).

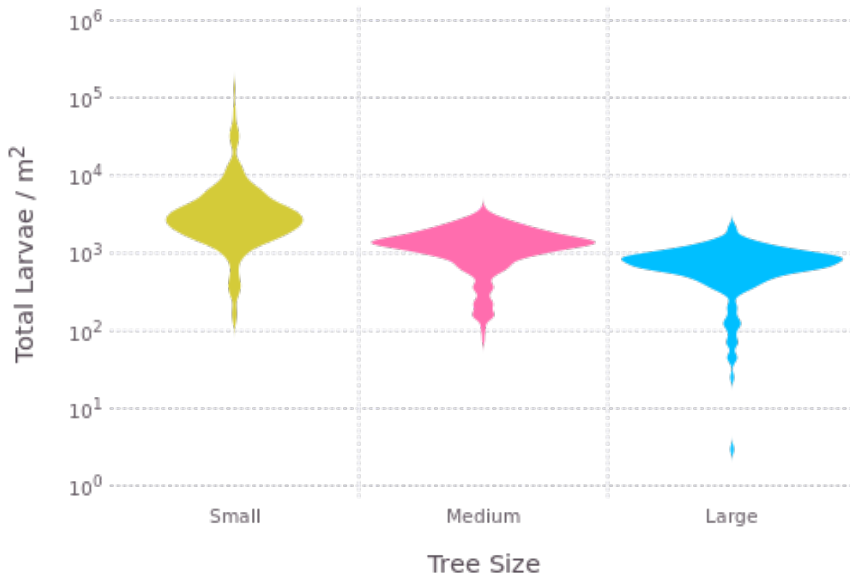
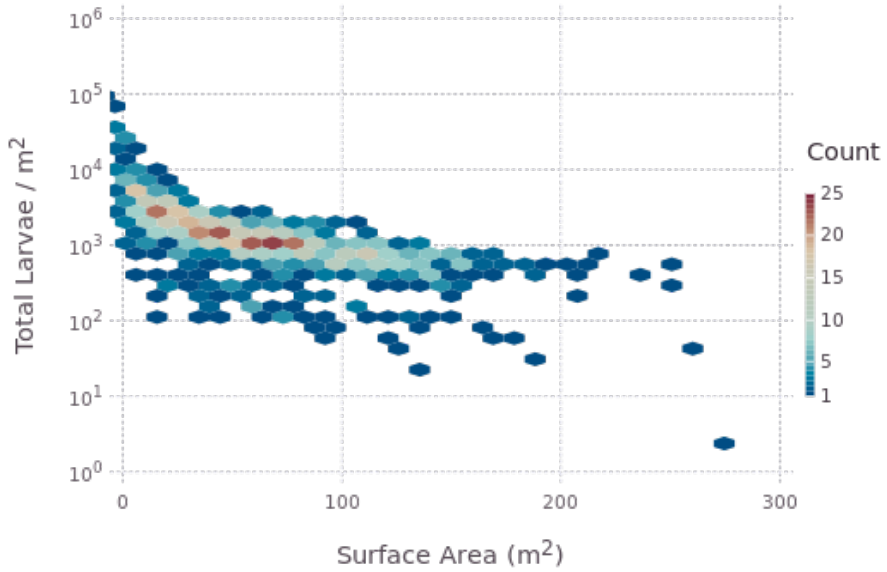


Figure 14: Distribution of the cumulative larval density and a tree's surface area when $\chi = 2$. In the bottom figure, trees have been placed into size groups based on their surface area: small, medium ($> 50 \text{ m}^2$), and large ($> 100 \text{ m}^2$).

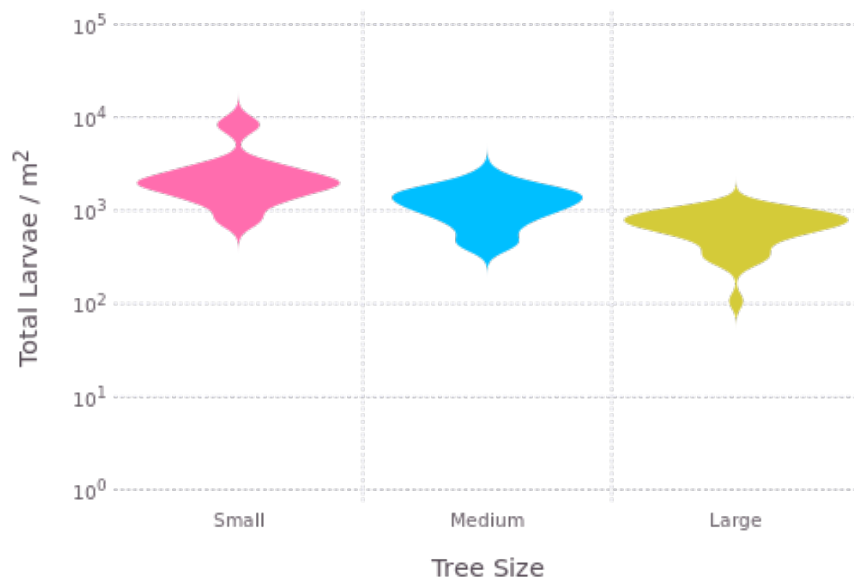
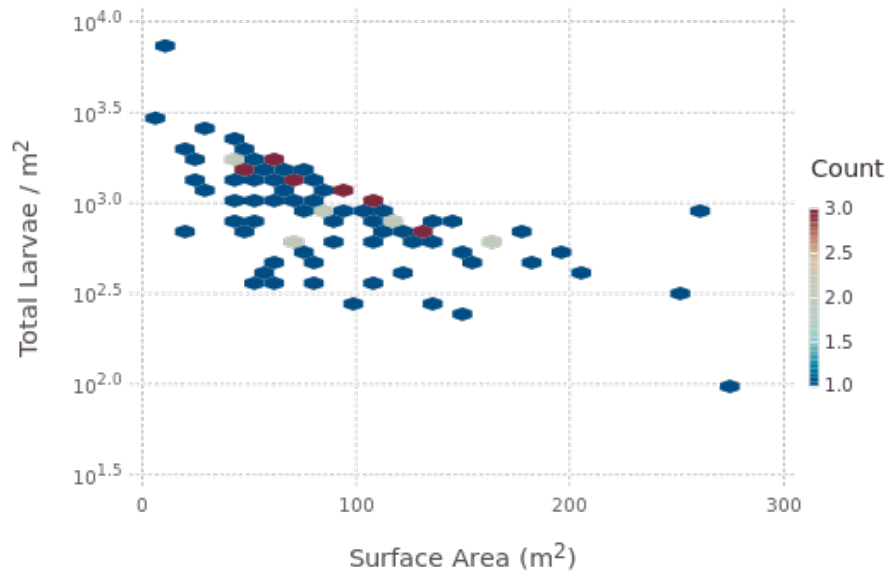


Figure 15: Distribution of the cumulative larval density and a tree's surface area when $\chi = 3$. In the bottom figure, trees have been placed into size groups based on their surface area: small, medium ($> 50 \text{ m}^2$), and large ($> 100 \text{ m}^2$).

Conclusion

This project set out to provide a basic model of how the emerald ash borer infestation spreads from an original infestation. Using agent-based modeling, the location and status of female EABs and ash trees are continuously monitored, with females moving from one ash to another as they lay eggs and infested new trees. The larvae can undergo several death-related events, before pupating into adults and beginning the process over again.

Overall, the simulation was able to produce estimates that were within a reasonable range compared to the observed values. Smaller trees appeared to be attacked too often as evidenced by their greater larval densities. Instead of focusing on weighting by the amount of surface area, one could weight by the amount of remaining surface area to account for previous infestations. This, however, would require some additional assumptions, and thus wasn't pursued in this paper.

A more advanced model could follow the basics of decision theory, such as done in [Anulewicz et al. \[2008\]](#). This could take additional considerations into mind, such as larval densities, the status of the tree, and the type of ash. This, however, leads to a drastic increase in the number of parameter to consider, and would require real-world data of the spread of the emerald ash borer with which to compare.

Bibliography

- T. Anderson and S. Dragicevic. An agent-based modeling approach to represent infestation dynamics of the emerald ash borer beetle. *Ecological Informatics*, 30:97–109, 2015.
- A. C. Anulewicz, D. G. McCullough, D. L. Cappaert, and T. M. Poland. Host range of the emerald ash borer (*agrilus planipennis fairmaire*) (coleoptera: Buprestidae) in north america: Results of multiple-choice field experiments. *Environmental Entomology*, 37(1):230–241, 2008. doi: 10.1603/0046-225X(2008)37[230:HROTEA]2.0.CO;2. URL [http://dx.doi.org/10.1603/0046-225X\(2008\)37\[230:HROTEA\]2.0.CO;2](http://dx.doi.org/10.1603/0046-225X(2008)37[230:HROTEA]2.0.CO;2).
- T. BenDor, S. Metcalf, L. Fontenot, B. Sangunett, and B. Hannon. Modeling the spread of the emerald ash borer. *Ecological Modelling*, 197(1-2):221–236, 8 2006. ISSN 0304-3800. doi: 10.1016/j.ecolmodel.2006.03.003.
- J. Bezanson, S. Karpinski, V. B. Shah, and A. Edelman. Julia: A Fast Dynamic Language for Technical Computing. *arXiv e-prints*, art. arXiv:1209.5145, Sept. 2012.
- J. Buck. Emerald ash borer program manual, 2015. URL https://www.aphis.usda.gov/import_export/plants/manuals/domestic/downloads/emerald_ash_borer_manual.pdf.
- D. Cappaert, D. G. McCullough, T. M. Poland, and N. W. Siegert. Emerald ash borer in north america: A research and regulatory challenge. *American Entomologist*, 51(3):152–165, 2005. doi: 10.1093/ae/51.3.152. URL <http://dx.doi.org/10.1093/ae/51.3.152>.
- R. A. Haack, Y. Baranchikov, L. S. Bauer, and T. M. Poland. Emerald ash borer biology and invasion history, 2015. URL https://www.fs.fed.us/nrs/pubs/jrnls/2015/nrs_2015_haack_001.pdf.

- D. A. Herms and D. G. McCullough. Emerald ash borer invasion of north america: History, biology, ecology, impacts, and management. *Annual Review of Entomology*, 59(1):13–30, 2014. doi: 10.1146/annurev-ento-011613-162051. URL <https://doi.org/10.1146/annurev-ento-011613-162051>. PMID: 24112110.
- D. McCullough and N. Siegert. Estimating potential emerald ash borer (coleoptera: Buprestidae) populations using ash inventory data. *Journal of economic entomology*, 100:1577–86, 10 2007. doi: 10.1603/0022-0493(2007)100[1577:EPEABC]2.0.CO;2.
- H. A. Mooney and E. E. Cleland. The evolutionary impact of invasive species. *Proceedings of the National Academy of Sciences*, 98(10):5446–5451, 2001. ISSN 0027-8424. doi: 10.1073/pnas.091093398. URL <https://www.pnas.org/content/98/10/5446>.
- T. Poland and D. Mccullough. Emerald ash borer: Invasion of the urban forest and the threat to north america’s ash resource. *Journal of Forestry*, 104: 118–124, 04 2006.
- A. Prasad, L. Iverson, M. Peters, J. Bossenbroek, S. N. Matthews, T. Sydnor, and M. Schwartz. Modeling the invasive emerald ash borer risk of spread using a spatially explicit cellular model. *Landscape Ecology*, 25:353–369, 03 2009. doi: 10.1007/s10980-009-9434-9.
- E. J. Rebek, D. A. Herms, and D. R. Smitley. Interspecific variation in resistance to emerald ash borer (coleoptera: Buprestidae) among north american and asian ash (*fraxinus* spp.). *Environmental Entomology*, 37(1):242–246, 2008. doi: 10.1603/0046-225X(2008)37[242:IVIRTE]2.0.CO;2. URL [http://dx.doi.org/10.1603/0046-225X\(2008\)37\[242:IVIRTE\]2.0.CO;2](http://dx.doi.org/10.1603/0046-225X(2008)37[242:IVIRTE]2.0.CO;2).
- A. Santini and M. Faccoli. Dutch elm disease and elm bark beetles: a century of association. *iForest - Biogeosciences and Forestry*, (2):126–134, 2015. doi: 10.3832/ifor1231-008. URL <http://iforest.sisef.org/contents/?id=ifor1231-008>.
- R. Taylor, T. Poland, L. Bauer, K. Windell, and J. Kautz. Emerald ash borer flight estimates revised. *Proceedings of the emerald ash borer/Asian longhorned beetle research and Te. FHTET-2007-04*, pages 10–12, 01 2007.